

Surface Analysis of PEGylated Nano-Shields on Nanoparticles Installed by Hydrophobic Anchors

M. F. Ebbesen · B. Whitehead · B. Ballarin-Gonzalez · P. Kingshott · K. A. Howard

Received: 30 December 2012 / Accepted: 1 March 2013 / Published online: 12 April 2013
© Springer Science+Business Media New York 2013

ABSTRACT

Purpose This work describes a method for functionalisation of nanoparticle surfaces with hydrophilic “nano-shields” and the application of advanced surface characterisation to determine PEG amount and accumulation at the outmost 10 nm surface that is the predominant factor in determining protein and cellular interactions.

Methods Poly(lactic-co-glycolic acid) (PLGA) nanoparticles were prepared with a hydrophilic PEGylated “nano-shield” inserted at different levels by hydrophobic anchoring using either a phospholipid-PEG conjugate or the copolymer PLGA-block-PEG by an emulsification/diffusion method. Surface and bulk analysis was performed including X-ray photoelectron spectroscopy (XPS), nuclear magnetic resonance spectroscopy (NMR) and zeta potential. Cellular uptake was investigated in RAW 264.7 macrophages by flow cytometry.

Results Sub-micron nanoparticles were formed and the combination of (NMR) and XPS revealed increasing PEG levels at the particle surface at higher PLGA-b-PEG copolymer levels. Reduced cellular interaction with RAW 264.7 cells was demonstrated that correlated with greater surface presentation of PEG.

Conclusion This work demonstrates a versatile procedure for decorating nanoparticle surfaces with hydrophilic “nano-shields”. XPS in combination with NMR enabled precise determination of PEG at the outmost surface to predict and optimize the biological performance of nanoparticle-based drug delivery.

KEY WORDS nanoparticles · PEG · stealth · surface analysis · XPS

INTRODUCTION

The utilisation of polyester poly(lactic-co-glycolic acid) (PLGA) for nanoparticle-based drug delivery is attractive due to its biocompatible and biodegradable properties (1,2) and FDA approval that has resulted in marketed sustained drug release systems based on subcutaneous or intramuscular injectable depots such as Zoladex (3) and Lupron (4). Increased plasma circulatory half-life of systemic particle-based drug delivery, however, remains a challenge and is a prerequisite for site-specific targeting (5). Functional modifications of the nanoparticle surface with hydrophilic polymers such as poly(ethylene glycol) (PEG) (6) is a strategy to reduce blood clearance mediated by the mononuclear phagocytic system (MPS).

Surface coatings can be performed either during, or post preparation of the particle. Post modification techniques include covalent conjugation and passive adsorption of shielding polymers to the particle surface. Conjugation is typically performed using reactive succinimide esters towards polymer amines or hydroxyls (7,8) thereby fixing the coating with covalent amide or ester bonds, however, the technique typically requires additional conjugation steps (6,9). Particle coatings with high surface density can generally be obtained by physisorption of Poloxamers or Poloxamines (10,11), however, this approach is limited by desorption of polymer from the surface (5,12) that can lead to non-coated regions onto which serum proteins (opsonins) can adsorb and facilitate macrophage recognition.

Protein adsorption to the particle surface is dependent on the graft density and thickness of the hydrophilic coating (13). Small proteins may penetrate a thin polymer coating and adsorb to the underlying substrate, whereas larger proteins may adsorb at the upper layers of a polymer coating if not sufficiently dense to screen long range interaction between

M. F. Ebbesen · B. Whitehead · B. Ballarin-Gonzalez ·
K. A. Howard (✉)
Interdisciplinary Nanoscience Center (iNANO)
Department of Molecular Biology and Genetics,
University of Aarhus Gustav Wieds Vej 14,
8000 Aarhus C, Denmark
e-mail: kenh@inano.au.dk

P. Kingshott
Industrial Research Institute Swinburne (IRIS)
Faculty of Engineering & Industrial Sciences,
Swinburne University of Technology
Hawthorn, Victoria 3122, Australia

protein and particle surface. The particle surface determines biological interactions, therefore, detailed analysis of the PEGylated “nano-shields” is crucial in determining the ability for rejecting protein interactions and the subsequent fate of the particle *in vivo* as well as to further optimise the system. The majority of reports in the literature have relied on the information gained from light/electron microscopy, light scattering and zeta potential measurements (6,14–16). Zeta analysis is non-quantitative and values vary dependent on pH and buffer resulting in literature inconsistencies. X-ray photoelectron spectroscopy (XPS) (17) is one of the few techniques with the relevant specificity and sensitivity and can provide information of the elemental composition and chemical state of the outermost 10 nm surface. Combined with nuclear magnetic resonance spectroscopy (NMR) it forms a strong toolset to gain a detailed composition of the particle coating.

Conjugation of PEG to a hydrophobic polymer such as PLGA creates a diblock copolymer with a natural tendency for partitioning at the hydrophilic/hydrophobic interface. This copolymer has been used in other types of particle formulations both as a coating agent (18) and as the particle matrix material (19,20), but often with the use of chlorinated solvents or high shear emulsification processes (21).

This work describes surface functionalisation of PLGA nanoparticles with PEG using hydrophobic anchorage with either phospholipids (1,2-distearoyl-sn-glycero-3-phosphoethanolamine-N-[methoxy(polyethylene glycol)] (PE-*b*-PEG) or PLGA polymer (PLGA-*block*-PEG). This was performed using a mild emulsion/diffusion preparation method that includes low stirring forces and the use of the non-chlorinated solvent benzyl alcohol (Fig. 1). It utilises a method previously used in our group for installation of a cetyl grafted poly(ethylene imine) (cetyl-PEI) as a surface coating agent for mediating delivery of siRNA (22). Detailed surface analysis was performed using XPS to determine the level of surface PEG, whilst NMR was used for total bulk PEG content. This allowed for assessing the extent to which PEG locates preferentially at the particle surface. The effect of surface PEG levels on cellular uptake was investigated in a RAW 264.7 macrophage cell line by flow cytometry.

MATERIALS AND METHODS

Materials

Poly(lactic-*co*-glycolic acid)-*block*-poly(ethylene glycol) (10,000:5,000) (PLGA-*b*-PEG) was purchased from Akina Inc. (USA) and was reprecipitated in diethyl ether from a DCM solution before use. Poly(lactic-*co*-glycolic acid) (PLGA, 13 kDa, Medisorb 2A, L/G ratio 53:47) was

obtained from Alkermes (USA). 1,2-distearoyl-sn-glycero-3-phosphoethanolamine-N-[methoxy(polyethylene glycol)-5000] (PE-*b*-PEG) was purchased from Avanti Polar Lipids (USA) and near infrared (NIR) fluorescent dye (ATTO 647 N) from Atto Tec (Germany). Benzyl alcohol, poly(ethylene glycol) (5 kDa) (non-anchoring PEG), poly(vinyl alcohol) (PVA, 13–23 kDa, 87–89% hydrolysed), Thiazolyl Blue Tetrazolium Bromide (MTT), Dulbeccos Phosphate Buffered Saline (PBS), RPMI media, DMEM glutamax, foetal bovine serum (FBS), penicillin and streptomycin (P/S) were purchased from Sigma Aldrich (USA). Ultrapure water (18 M Ω) from an ELGA PURELAB flex was used in all experiments.

Particle Preparation

Nanoparticles were prepared using a modified emulsion emulsification/diffusion method (22) (Fig. 1). A filtered (0.2 μ m) solution (50 mg/ml, 1 mL) of PLGA in benzyl alcohol (BA) was mixed with 100 μ L of a BA solution with PE-*b*-PEG, PLGA-*b*-PEG (0, 6 or 30%*w/w* to PLGA) or non-anchoring PEG as control (30%*w/w* to PLGA) either with or without a NIR fluorescent dye (10 μ L, 5 mg/mL in BA) in a flat bottomed glass stirring vial. The solution was emulsified with an aqueous, filtered (0.45 μ m filter) PVA solution (2.2 mL, 10%*w/w*) added over 2 min whilst stirring at 1800 rpm with a PTFE paddle (BOLA, Germany) (Fig. 1a). The stirring was continued for 2 min. The BA was then extracted from the emulsion droplets by adding 34 mL of water over 10 min and stirring for an additional 15 min (Fig. 1b). The particles were pelleted by centrifugation (4°C, 10 min., rcf 4,000 g) and washed first, with a dilute PVA solution (0.5%*w/w*) and second, with water (Fig. 1c). The particles were resuspended in 10 mL of ddH₂O and aliquots were taken for scanning electron microscopy (SEM) visualisation and XPS analysis. The remaining sample was frozen on liquid nitrogen in 1 mL aliquots with the addition of sucrose as cryoprotectant as a concentration of 50 mg/mL. Particles were freeze-dried at 0.012 Torr in 48 h at room temperature.

Evaluation of Particle Size, Charge and Morphology

Zeta potential and hydrodynamic particle diameter were measured in triplicates with a Zetasizer Nano ZS, Malvern (UK) in 10 mM HEPES buffer (pH 7.0) at 25°C. In addition zeta potentials were also measured either in water, 10 mM sodium acetate (pH 5.5) or 10 mM sodium borate (pH 9) (Table II). For the SEM imaging, particles were air-dried onto aluminum stubs (Electron Microscopy Sciences) and subsequently sputter coated with gold (1.25 kV, 2 min).

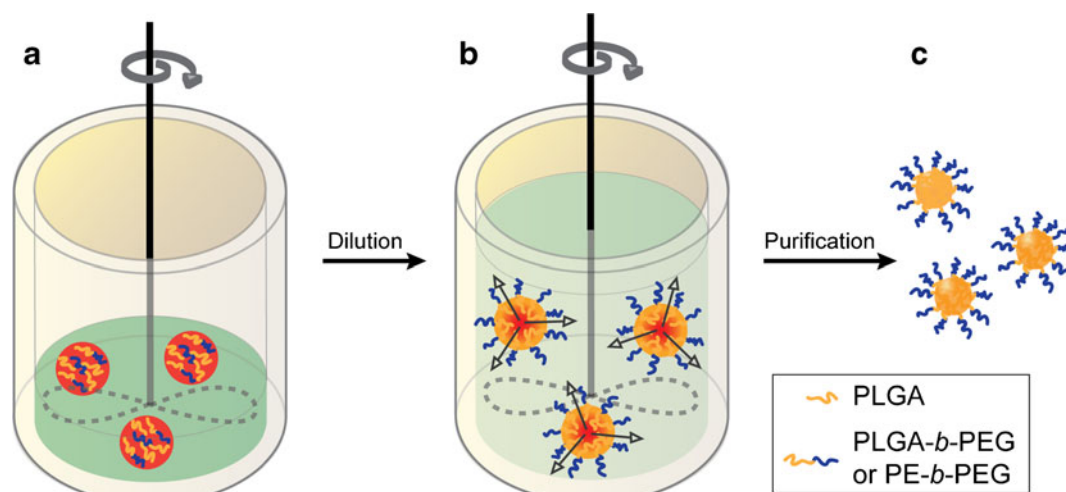


Fig. 1 PEGylated PLGA nanoparticle preparation using an emulsion solvent-diffusion method. PLGA in benzyl alcohol (BA) with either PE-*b*-PEG or PLGA-*b*-PEG was emulsified with an aqueous PVA solution to form droplets (a). Subsequently BA was removed by dilution of the emulsion with water (b). After purification, PEGylated PLGA particles were obtained (c).

SEM analysis was performed using a NOVASEM in high vacuum mode.

X-ray Photoelectron Spectroscopy for Determination of Surface PEG

Samples were washed 2 times with water as for particle preparation. XPS samples were prepared by drying ~1 mg of particles on a clean aluminum XPS sample holder. Reference samples of pure polymer were deposited on XPS sample holders from an acetone solution. The analysis was performed using a Kratos AXIS Ultra^{DL} with a monochromated Al_{Kα} radiation source and photoelectron take-off angle of 0° to the surface normal operating at 10 mA emission current and 15 kV anode potential. Charge neutralization was achieved using the Kratos magnetic lens system. Survey spectra and high resolution scans of the C1s core level were obtained with a pass energy of 160 eV and 20 eV respectively and were both analysed using CasaXPS version 2.3.15 for determination of elemental compositions and C1s functional group (C-C/C-H (methylene carbon), C-O-C/C-OH (ether carbon), O-C-C(O) (alpha ester carbon) and C(O)O (ester carbon)) compositions on the particle surface. The constraints used for fitting were in general a FWHM of 1.4 eV and a C-O-C/C-OH peak position of between 286.5 and 285.8 eV. Shirley background subtraction was used for all spectra.

Determination of Dye and Bulk PEG Content

Particles were washed, vacuum dried and dissolved in deuterated chloroform by using sonication for 15 min. This solution containing the dissolved PLGA-, block

copolymer-, PEG-components and dye (ATTO 647 N) was filtrated through PTFE syringe filters (0.20 μm, Sartorius Stedim) to remove any non-dissolved PVA. PEG incorporation into particle bulk was measured by ¹H-NMR on a Varian FT NMR spectrometer. The dye-related absorbance was measured at 644 nm in a quartz cuvette using a NanoPhotometer (IMPLEN) (Fig. 5).

Cellular Uptake and Viability Studies

Cell uptake studies were performed in the murine macrophage RAW 264.7 cell line. Cells were maintained at 37°C with 5% CO₂ in DMEM Glutamax medium supplemented with 10% foetal bovine serum and 1% Pen/Strep. Cells were passaged by mechanical detachment (cell scraper) at 1:6. Cells were seeded at concentrations of 3·10⁵ cells/well in 1 mL medium in a 24-well plate. Twenty four hours later the medium was replaced with 250 μL of medium (+/- serum) containing particles at a concentration of 0.4 mg/mL. After 2.5 h particles and medium was removed followed by a PBS wash and the cells removed by mechanically scraping and centrifuged at 300 g for 10 min. A PBS wash was repeated and cells were resuspended in 0.5 mL 2% FBS/PBS and kept in the dark until flow analysis.

Flow cytometry was performed using a Gallios (Beckman Coulter) flow cytometer using 635 nm laser and 660/20 nm filter. A minimum of 1,200 events were collected for each sample. Cell population selection was based on forward and side scattering, and the geometric mean value of three replicates of the FL6 channel histogram was used for quantification of cell uptake. The level of NIR associated cellular

fluorescence was determined using the geometric mean value of three replicates. Averages were normalised to cells treated with non-coated particles (0%*w/w* PLGA-*b*-PEG). Statistical changes in uptake was calculated using a *t*-test.

A tetrazolium based assay (MTT) was used to determine cell viability using the uptake study protocol repeated in 96 well plates. After particles/media were removed, 100 μ l MTT solution in RPMI media (0.5 mg/ml, free of phenol red) was added and the cells incubated at 37°C for ~45 min. The solution was removed and the converted dye solubilised with 100 μ l DMSO and the absorbance read at 570 nm with background subtraction at 650 nm. Results were normalised to absorbance of untreated cells and statistical changes were calculated using *t*-test.

RESULTS

Size and Morphology of PLGA Particles

Dynamic Light Scattering (DLS) (Table I) and SEM (Fig. 2) were used to measure the average hydrodynamic particle diameter and to evaluate the surface morphology of the particles respectively. SEM analysis showed some degree of polydispersity, but a size distribution from ~0.5 to 1.5 μ m was obtained which correlated to the hydrodynamic particle size measured by DLS. Discrete spherical particles with a smooth surface for both PLGA-*b*-PEG (Fig. 2c, d) and PE-*b*-PEG (Fig. 2e, f) systems were visualized. Particles formulated with the PE-*b*-PEG coating (Fig. 2e, f) showed a similar size and appearance to the blank particles (Fig. 2a), which was also evident from the DLS data with 6% PE-*b*-PEG coated particles having almost the same hydrodynamic radius as the blank particles.

Zeta (ζ) potential is the electric potential at a distance of a few nanometers away from the particle surface and is a

standard method to evaluate the surface functionalisation of particles. We show that the value is dependent on pH and ionic strength of the medium with the panel of particles in our work (Table II) which brings into question its usefulness as a standard method in light of the different buffer systems used in the literature. In our work, a general negative ζ -potential value indicated the presence of PLGA terminal carboxylic acid groups on the particle under all conditions as expected. Introduction of the PLGA-*b*-PEG coating reduced the ζ -potential value further for particles measured in water and in 10 mM buffer at pH 5.5 and 7.0. Particles measured in 10 mM borate buffer at pH 9.0 showed increased ζ -potential value when coated with PLGA-*b*-PEG. These results suggest zeta analysis in combination with other methods is required for reliable determination of particle functionalisation.

PEG Determination Using NMR Spectroscopy

NMR spectroscopy was performed to allow determination of the composition of the bulk particle with respect to the amounts of PEG ((OCH₂) at δ 3.64 ppm) to PLGA ((C(O)CH₂) at δ 4.82 ppm) (Fig. 3). Spectra showed little or no evidence of PEG for particles prepared with copolymers PE-*b*-PEG which matched the 0% (blank) and 30% non-anchoring PEG samples. The lack of PEG in the 30% non-anchoring PEG control supports the necessity for an anchor to enable installation of PEG onto the particle. The lack of PEG in the PE-*b*-PEG system suggests insufficient anchoring.

Incorporation of PLGA-*b*-PEG in the particles was quantified by integration of the NMR spectra. Peaks of PLGA (galactic acid methylene protons) were normalised to unity, and PEG peaks thus integrated to the values 0.08 and 0.31 for the 6% and 30% PLGA-*b*-PEG samples respectively. The theoretical molar ratio of PEG to PLGA repeat units in the particles can be calculated to 0.06 and 0.26 for the 6% and 30% PLGA-*b*-PEG samples respectively. Taking the numbers of protons on the PEG and galactic acid units into account it, thus, correlates with the values of 0.08 and 0.31 and indicates incorporation of 66% and 59% of PLGA-*b*-PEG into the particles for the 6% and 30% PLGA-*b*-PEG samples respectively.

Surface PEG Determined by X-ray Photoelectron Spectroscopy

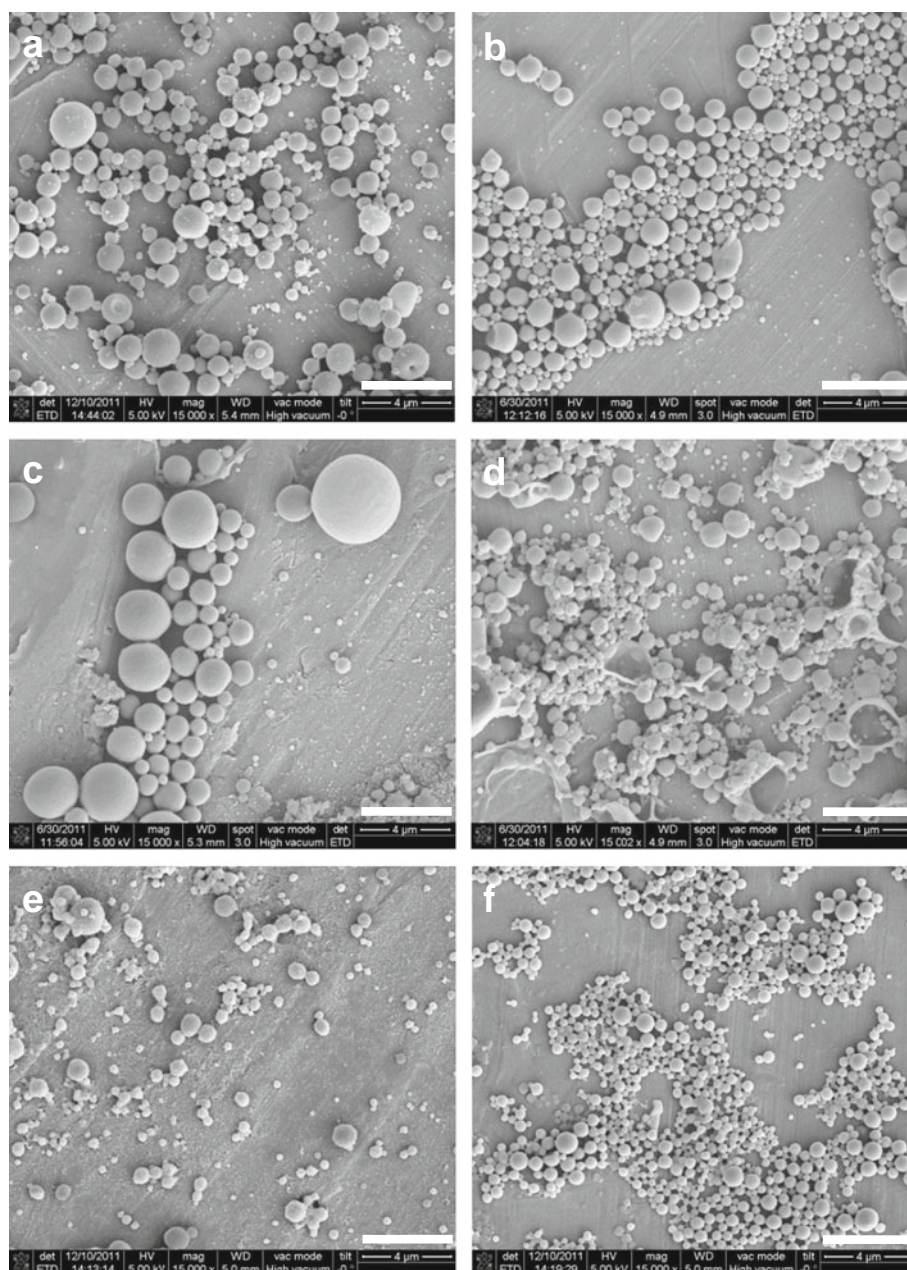
XPS analysis showed a consistent elemental composition with all the particle formulations, whereas the detailed chemical state information in the C1s spectra revealed the changing surface chemistries. A precise measure of the amount of surface PEG from the PLGA-*b*-PEG copolymer was made by curve-fitting the C1s spectra into the four

Table I Hydrodynamic Size (Z-av), Pdl and Zeta Potential (ζ) of Particles Resuspended in 10 mM HEPES Buffer pH 7.0

Sample	Z-av [d.nm]	Pdl	ζ (HEPES pH7.0)
0% (blank)	743	0.44	-5.8 (\pm 0.3)
30% n.a. PEG	1092	0.66	-6.5 (\pm 0.2)
6% PLGA- <i>b</i> -PEG	1293	0.75	-10.7 (\pm 0.6)
30% PLGA- <i>b</i> -PEG	1039	0.60	-13.1 (\pm 0.4)
6% PE- <i>b</i> -PEG	765	0.57	-6.7 (\pm 0.1)
30% PE- <i>b</i> -PEG	1036	0.74	-6.5 (\pm 0.3)

The average of three measurements is displayed and standard deviation for ζ -potential value given in brackets. "n.a. PEG" abbreviates non-anchoring PEG

Fig. 2 Scanning electron microscopy (SEM) images of particles. Particles were deposited onto aluminium SEM stubs and air-dried before SEM analysis. **(a)** 0% (blank), **(b)** 30% non-anchoring PEG, **(c)** and **(d)** 6% and 30% PLGA-*b*-PEG, **(e)** and **(f)** 6% and 30% PE-*b*-PEG. Bar on image correspond to 4 μ m.



peaks $\underline{\text{C}}\text{-C}/\underline{\text{C}}\text{-H}$ at 285.0 eV, $\underline{\text{C}}\text{-O-C}/\underline{\text{C}}\text{-OH}$ at 286.2 eV, $\text{O-}\underline{\text{C}}\text{-C}(\text{O})$ at 287.2 eV and $\underline{\text{C}}(\text{O})\text{O}$ at 289.4 eV (Fig. 4). The elemental and C1s chemical species composition are presented in Table III.

The analysis of the basic polymer components shows how the different C1s environments vary dependent on the polymer (Table III, A). Three different environments are shown for PLGA, which corresponds to the $\underline{\text{C}}\text{-C}/\underline{\text{C}}\text{-H}$ (methylene

Table II Zeta Potential (ζ) of Particles Measured in Different Buffer Conditions

Sample	ζ (NaAc pH 5.5)	ζ (HEPES pH 7.0)	ζ (NaBorate pH 9.0)	ζ (water)
0% (blank)	-1.3 (± 0.1)	-5.4 (± 0.2)	-17.0 (± 0.3)	-25.9 (± 3.7)
6% PLGA- <i>b</i> -PEG	-3.3 (± 0.1)	-10.7 (± 0.6)	-5.9 (± 0.2)	-31.2 (± 0.3)
30% PLGA- <i>b</i> -PEG	-3.7 (± 0.1)	-13.1 (± 0.4)	-4.8 (± 0.1)	-44.2 (± 1.3)

All measuring medias except water contained 10 mM concentration of the buffer components. The average of three measurements is displayed and standard deviation given in brackets

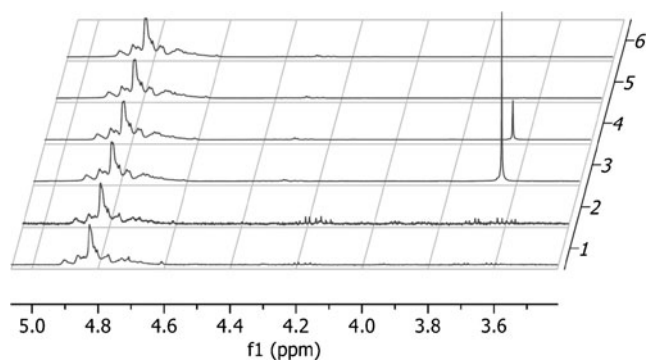


Fig. 3 NMR spectra of particles measured in deuterated chloroform. 30% and 6% PE-*b*-PEG (lanes 1 and 2), 30% and 6% PLGA-*b*-PEG (lanes 3 and 4), 30% non-anchoring PEG (lane 5) and 0% (blank) (lane 6). The peak from the galactic acid methylene protons (δ 4.82 ppm) is seen in all spectra, whereas the peak from PEG (δ 3.64 ppm) is only seen in samples with 30% and 6% PLGA-*b*-PEG.

carbon), O- $\underline{\text{C}}$ -C(O) (α ester carbon) and $\underline{\text{C}}$ (O)O (ester carbon) groups. The C1s $\underline{\text{C}}$ -O-C/ $\underline{\text{C}}$ -OH (ether carbon) peak relates to PEG and PVA and the analysis of the basic polymer components show how this level changes in PLGA-*b*-PEG, PE-*b*-PEG, non-anchoring PEG and PVA (Table III, A). XPS survey spectra revealed only carbon and oxygen elemental species to be present in the outermost 10 nm particle surface as expected, and the changing amount of surface PEG was reflected in the level of the ether carbon C1s chemical specie ($\underline{\text{C}}$ -O-C/ $\underline{\text{C}}$ -OH) for each particle formulation (Table III, B). The surface $\underline{\text{C}}$ -O-C/ $\underline{\text{C}}$ -OH content for the PLGA-*b*-PEG coated particles increased from 5.9% (0% (blank)) to 11.6% and 15.6% (6% and 30%

PLGA-*b*-PEG, respectively) reflecting the change in coating concentration. This $\underline{\text{C}}$ -O-C/ $\underline{\text{C}}$ -OH level seemed considerably higher compared to the PE-*b*-PEG particles (5.4% and 3.1%) which provided additional evidence that the phospholipid anchor did not interact with PLGA in the particles to the same extent as the PLGA anchor.

Comparing the NMR and XPS data, it is possible to determine the degree to which the PLGA-*b*-PEG accumulates at the particle surface or if the surface amounts equals that of the bulk (Table IV). The particle bulk $\underline{\text{C}}$ -O-C/ $\underline{\text{C}}$ -OH content can be estimated from the $\underline{\text{C}}$ -O-C/ $\underline{\text{C}}$ -OH level of PLGA-*b*-PEG as measured on the basic polymer components (Table III, A) and the PLGA-*b*-PEG incorporation level as measured by NMR. Comparing this to the particle surface $\underline{\text{C}}$ -O-C/ $\underline{\text{C}}$ -OH content measured by XPS, surface to bulk ratios of 9.7 and 3.5 were found for 6% and 30% PLGA-*b*-PEG, respectively (Table IV).

Cellular Uptake and Viability Studies

Cellular particle uptake was quantified by the level of dye related fluorescence measured by flow cytometry, so similar particle dye content is needed for these studies. This was quantified by measuring the dye related absorbance at 644 nm (Fig. 5). The amount of dye was similar for each sample except those prepared with PE-*b*-PEG polymers. This could either indicate insufficient dye incorporation into PLGA particle core or that the yield of particles prepared with these polymers was low. On the basis of this, and the XPS and NMR data, it was decided to investigate the effect of PEGylation by cellular uptake only with the PLGA-*b*-PEG particles.

The PLGA-*b*-PEG coated particles showed a significant decrease in cellular uptake when increasing the PLGA-*b*-PEG content from 0% (blank) to 6% (decrease of 46% with serum, 34% without serum, $P < 0.005$) and from 6% to 30% (decrease of 27% with serum and 12% without serum, $P < 0.05$). In total, a decrease in uptake up to 68% and 74% was observed dependent on serum presence (Fig. 6). Raising the serum percentage from 0% to 10% resulted in significant increased particle uptake for non-PEGylated formulations (22% and 32% increase for 0% (blank) and 30% non-anchoring PEG, respectively, $P < 0.05$) compared to the PEGylated formulations (6% and 30% PLGA-*b*-PEG), which were not significantly affected.

The viability of the RAW 264.7 cell line in the presence of particles at the same concentration as the uptake studies was investigated (Fig. 7). Cells treated with PLGA-*b*-PEG, non-anchoring PEG and blank particles displayed cell viabilities that were not statistically different compared to non-treated cells (P between 0.10 and 0.98) that suggest no detrimental effects of the PLGA-*b*-PEG copolymer coated particles.

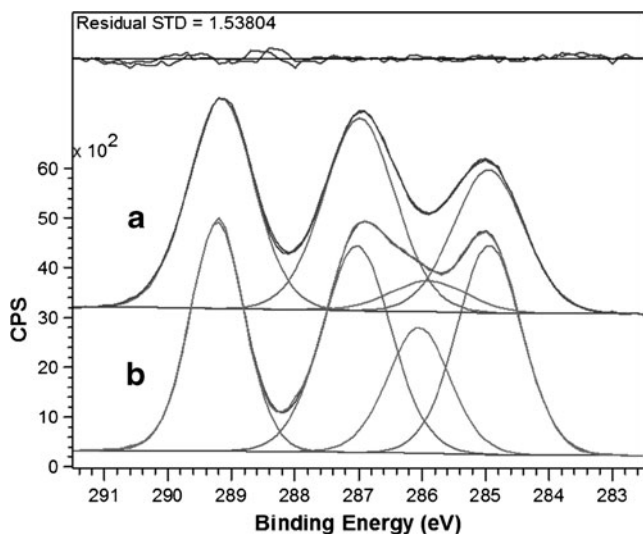


Fig. 4 Decomposed XPS C1s spectrum of particles coated with (a) 0% PLGA-*b*-PEG and (b) 30% PLGA-*b*-PEG. The position of the four C1s components are: $\underline{\text{C}}$ -C/C-H at 285.0 eV, $\underline{\text{C}}$ -O-C/ $\underline{\text{C}}$ -OH at 286.2 eV, O- $\underline{\text{C}}$ -C(O) at 287.2 eV and $\underline{\text{C}}$ (O)O at 289.4 eV.

Table III XPS Analysis of the Relevant Basic Components and of the Different Coated Nanoparticle Formulations

	C 1s spectra composition (%)				Elemental composition (%)	
	<u>C</u> (O)O	O- <u>C</u> -C(O)	<u>C</u> -O-C/ <u>C</u> -OH	<u>C</u> -C/ <u>C</u> -H	C	O
A) Basic components						
PLGA	38.0 (±1.0)	38.9 (±0.5)	0.1 (±0.1)	23.1 (±0.5)	59.3 (±0.1)	40.7 (±0.1)
n.a. PEG	0.0 (±0.0)	0.0 (±0.0)	93.3 (±1.3)	6.7 (±1.3)	70.5 (±0.3)	29.5 (±0.3)
PLGA- <i>b</i> -PEG	21.8 (±1.8)	22.0 (±2.0)	29.5 (±2.5)	26.6 (±3.3)	65.5 (±1.6)	34.4 (±1.7)
PE- <i>b</i> -PEG	2.5 (±0.2)	7.3 (±2.4)	64.0 (±7.1)	26.1 (±4.5)	74.8 (±0.3)	24.7 (±0.2)
PVA	12.6 (±0.7)	0.0 (±0.0)	47.0 (±0.9)	40.4 (±0.9)	68.4 (±0.2)	31.6 (±0.2)
B) Formulations						
0% (blank)	34.2 (±0.2)	34.2 (±0.4)	5.9 (±0.5)	25.8 (±0.9)	59.6 (±0.5)	40.4 (±0.5)
30% n.a. PEG	36.9 (±0.1)	37.0 (±0.5)	1.3 (±0.0)	24.8 (±0.5)	59.4 (±1.0)	40.7 (±1.0)
6% PLGA- <i>b</i> -PEG	29.4 (±1.8)	32.9 (±1.8)	11.6 (±4.1)	26.2 (±0.6)	60.6 (±0.2)	39.4 (±0.2)
30% PLGA- <i>b</i> -PEG	26.4 (±0.6)	29.4 (±3.4)	15.6 (±5.0)	28.6 (±1.4)	60.7 (±0.3)	39.3 (±0.3)
6% PE- <i>b</i> -PEG	34.9 (±0.9)	35.0 (±1.4)	5.4 (±1.5)	24.7 (±1.1)	59.0 (±0.7)	41.0 (±0.7)
30% PE- <i>b</i> -PEG	35.1 (±1.3)	36.1 (±0.6)	3.1 (±1.0)	25.7 (±1.6)	59.4 (±0.5)	40.6 (±0.5)

The average of three measurements is displayed and standard deviation given in brackets. "n.a. PEG" abbreviates non-anchoring PEG

DISCUSSION

In this work we investigated the capability of two different hydrophobic anchored PEG copolymers to introduce a PEGylated nano-shield onto the surface of PLGA particles using a novel emulsification/diffusion process. Advanced surface characterisation was provided by x-ray photoelectron spectroscopy to determine PEG in the outer 10 nm layer, whilst, NMR was used for bulk determination. In combination, we were able to investigate the accumulation of PEG at the particle surface. The PLGA-*b*-PEG copolymer was identified as the most effective material for enshrouding the particles and its biological effect confirmed by reducing phagocytic capture by macrophages.

The particles were coated by an emulsification/diffusion process previously used in our group for the incorporation of cetyl-PEI with the cetyl group acting as a hydrophobic anchor in the PLGA matrix (22). As an extension of this method, we compared the effect of using PEG with different

anchors constituted by either a PEGylated phospholipid or PLGA-*b*-PEG copolymer. PLGA-*b*-PEG has previously been used as a surface coating agent by utilising PLGA for hydrophobic anchorage into the PLGA particle matrix (18). The phospholipid PE-*b*-PEG has mainly been used with micellar nanocarriers (23,24) with limited use as a PLGA particle coating material (15). However, in contrast to these and other reports, our work addresses precise quantification of PEG presented on the surface of particles in combination with production using a novel emulsification/diffusion technique using mild stirring and non-toxic solvents.

SEM analysis showed particles with either the PE-*b*-PEG or PLGA-*b*-PEG to have a smooth surface morphology and a size range from ~0.5 to 1.5 µm that correlated with the DLS data. PLGA particles formulated with 6 and 30%

Table IV Evaluation of the PEG Amounts in the Particle Bulk (NMR) and on the Particle Surface (XPS)

Formulations	<u>C</u> -O-C/ <u>C</u> -OH component percentage (%)		
	NMR (bulk)	XPS (surface)	Ratio
6% PLGA- <i>b</i> -PEG	1.2	11.6 (±4.1)	9.7
30% PLGA- <i>b</i> -PEG	4.5	15.6 (±5.0)	3.5

The NMR-based estimate of the C-O-C/C-OH component percentage of the particle bulk is shown together with the surface C-O-C/C-OH component percentage measured by XPS. The ratio denotes the fold surface enrichment of PEG compared to the particle bulk

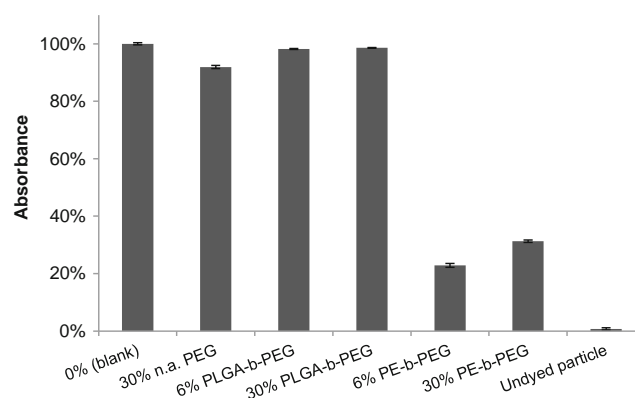


Fig. 5 Quantification of particle dye content. Particles were dissolved in chloroform, filtrated and the dye-related absorbance measured at 644 nm. Absorbance values shown are normalized to the 0% blank particle formulation. "n.a. PEG" abbreviates non-anchoring PEG. Error bars represent Standard Deviation.

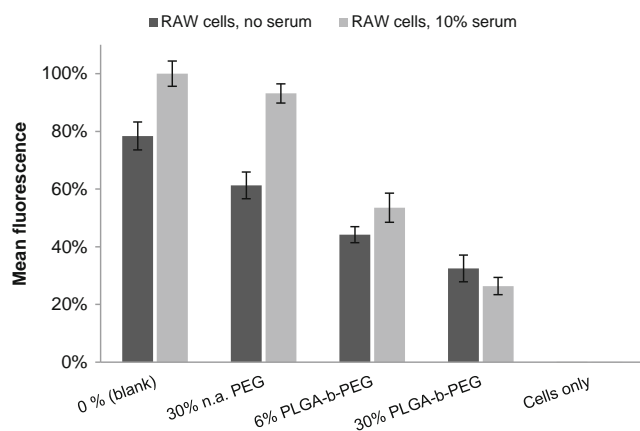


Fig. 6 Particle uptake in the RAW 264.7 cell line based on cellular associated fluorescence. Dye loaded particles were added to cells and incubated for 2.5 h, the cells were then washed twice and removed. Flow cytometry and analysis was performed to evaluate the level of particle uptake based on the geometric mean value of three replicates. Averages were normalized to cells treated with non-coated particles (0%w/w PLGA-*b*-PEG). PLGA-*b*-PEG coated particles showed a significant decrease in cellular uptake with increasing PLGA-*b*-PEG content, $P < 0.05$. "n.a. PEG" abbreviates non-anchoring PEG. Error bars represent Standard Deviation.

PE-*b*-PEG showed very similar size to the blank particles whereas the PLGA-*b*-PEG material at 6 and 30% coating seemed to increase particle size that indicates different incorporation effects of the PLGA-*b*-PEG compared to the PE-*b*-PEG.

Our findings demonstrate that PLGA particle ζ -potential is heavily influenced by pH and ionic strength. As the PLGA polymer has terminal carboxylic acid groups, grafting of a neutral, hydrophilic polymer such as PEG onto a PLGA particle surface should lead to ζ -potential values going from negative (0% (blank)) towards neutral (6% and 30% PLGA-

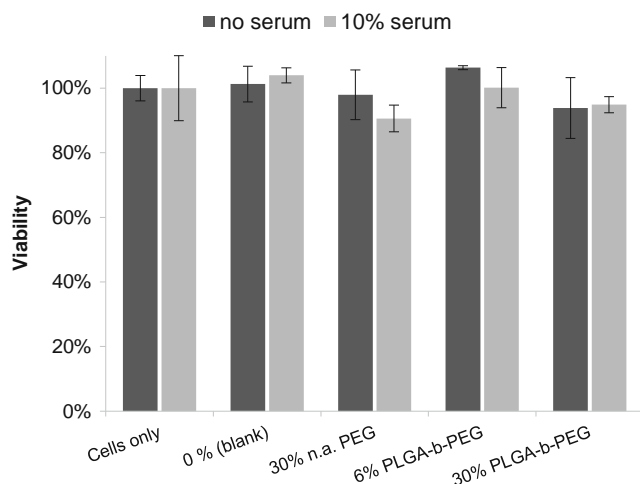


Fig. 7 RAW 264.7 cell viability using an MTT assay after incubation with coated and non-coated PLGA particles. Results were normalised to untreated cells. Measured cell viabilities with particles were not significantly different from the untreated control, P was between 0.10 and 0.98. "n.a. PEG" abbreviates non-anchoring PEG. Error bars represent Standard Deviation.

b-PEG). However, for buffers at pH 5.5 and pH 7.0 and in water, the ζ -potential potential changed to more negative values with increased coating material (Table II), which is seen in other work on PEG modified PLGA particles (6,14,15). Measuring at pH 9.0 the trend reverses to what would be expected (Table II). In a non-buffered system, such as pure water, pH easily fluctuates which affects the ζ -potential substantially as demonstrated in Table II. Consequently pure non-buffered water is not a good medium for ζ -potential measurements, but is, however, often used as such (15). The ζ -potential magnitude for the non-modified particles changed over a broad range of pH values (5.5 to 9.0), that was probably due to the polyelectrolyte effect by which dissociation of COOH groups is more difficult whilst in close proximity to already dissociated COO⁻ groups, broadening the pK_a -value of surface COOH groups (25), which was supported by our findings (Table II). Zeta potential have quite often been reported without an accompanying measure of pH and strength of the used measuring buffer (16,19,26), which lead to an inconsistency in the literature. Altogether this clearly highlights the drawback for using ζ -potential alone for evaluation of particle coating processes. Therefore, a focus of our work was to demonstrate the importance of using combined XPS and NMR for a more precise surface characterisation.

The NMR and XPS data showed insufficient particle incorporation of PEG using the PE-*b*-PEG in comparison with PLGA-*b*-PEG. An explanation could be the tendency for the PLGA bulk polymer to mix better with a similar PLGA-*b*-PEG in contrast to the PE-*b*-PEG. Another explanation is micelle formation by the PE-*b*-PEG in an aqueous environment which could prevent availability for interaction with the PLGA particle surface (24). PE-*b*-PEG has, however, been used previously to coat small PLGA nanoparticles ~65 nm in diameter using a nanoprecipitation solvent (acetonitrile) evaporation technique (15) although, NMR or XPS were not used to determine PEG incorporation.

XPS showed that particles produced using 6% and 30% PLGA-*b*-PEG displayed a higher $\underline{C}-O-C/\underline{C}-OH$ surface content (11.6% and 15.6%, respectively) compared to the blank and 30% non-anchoring PEG particles (5.9% and 1.3% respectively) (Table III). $\underline{C}-O-C/\underline{C}-OH$ groups from PVA and PEG are difficult to distinguish in a XPS spectrum due to similar binding energies of 286.47 eV and 286.45 eV respectively and so a C1s ether component here could be ambiguous if complimentary characterization methods had not been used. NMR was used for quantifying total PEG content in the particles on basis of peak integration, and showed no PEG in blank, 30% non-anchoring PEG, 6% and 30% PE-*b*-PEG particles (Fig. 3).

Amphiphilic molecules such as PLGA-*b*-PEG should ideally locate on the water/oil interface in the emulsification

step and remain there, entangled with the core polymer, as the particle solidifies. The coating polymers PLGA-*b*-PEG and PE-*b*-PEG (and PEG) are, however, added in the benzyl alcohol oil phase and could consequently end up in the particle bulk as well, which could negatively impact PEG surface coverage (6). NMR and XPS were used in combination to estimate the extent to which the PLGA-*b*-PEG accumulates at the particle surface, something that is normally difficult to assess. The overall amount of the XPS PEG $\underline{\text{C}}\text{-O-C}/\underline{\text{C}}\text{-OH}$ component in the particle bulk is proportional to the bulk level of PEG, PE-*b*-PEG or PLGA-*b*-PEG polymers, and can, therefore, be estimated if these levels are known. The incorporation of PEG in the abovementioned forms can be quantified using NMR and thus the PEG $\underline{\text{C}}\text{-O-C}/\underline{\text{C}}\text{-OH}$ component percentage of the particle bulk can be estimated to 1.2% and 4.5% for the 6% and 30% PEG-*b*-PLGA formulation respectively (Table IV). The surface PEG content measured by XPS is up to 15.6% (Tables III and IV). A comparison of the PEG content on the surface and in the bulk shows that PEG does accumulate predominantly at the surface for these particles as the surface to bulk ratio is much higher than 1 (Table IV). It also suggests, that even though the 30% PLGA-*b*-PEG formulation displays the highest PEG coverage ($\underline{\text{C}}\text{-O-C}/\underline{\text{C}}\text{-OH}$ is 15.6%), the 6% PLGA-*b*-PEG formulation has most optimal PEG surface packing efficiency (surface to bulk ratio of 9.7, Table IV). These findings show that XPS and NMR are good complementary techniques for thorough particle characterisation, as in combination they are able to identify and quantify polymers on the surface and in the bulk of nanoparticles.

The PLGA-*b*-PEG coated particles showed a significant decrease in cellular uptake (~70%) that correlated with increased surface presentation of PEG following the increasing percentage of copolymer in the particle formulation (Fig. 6). Furthermore the particles were well tolerated by the macrophage cell line as none of the measured cell viabilities differed significantly from the control (P between 0.10 and 0.98) (Fig. 7).

This work describes a mild and efficient method for the surface functionalisation of PLGA particles with PEGylated nano-shields and determination of surface PEG presentation using a combination of NMR and XPS.

CONCLUSION

This work demonstrates the use of PLGA-*b*-PEG to install PEG onto the surface of PLGA particles produced by a simple emulsification/diffusion method without the use of chlorinated solvents. Advanced surface characterisation was provided by XPS to determine PEG in the outer 10 nm layer, whilst, NMR was used for bulk determination. This combination provides a more precise and reliable method than the commonly used ζ -potential technique that is

susceptible to variations in different pH and salt conditions. Reduction in phagocytic capture of nanoparticles correlated with increased PEG content.

ACKNOWLEDGMENTS AND DISCLOSURES

We thank the Lundbeck Foundation for supporting this work through the grant: Lundbeck Foundation Nanomedicine Center for Individualised Management of Tissue Damage and Regeneration.

REFERENCES

1. Cartiera MS, Johnson KM, Rajendran V, Caplan MJ, Saltzman WM. The uptake and intracellular fate of PLGA nanoparticles in epithelial cells. *Biomaterials*. 2009;30(14):2790–8.
2. Murakami H, Kobayashi M, Takeuchi H, Kawashima Y. Preparation of poly(DL-lactide-co-glycolide) nanoparticles by modified spontaneous emulsification solvent diffusion method. *Int J Pharm*. 1999;187(2):143–52.
3. Walker KJ, Turkes AO, Turkes A, Zwink R, Beacock C, Buck AC, et al. Treatment of patients with advanced cancer of the prostate using a slow-release (depot) formulation of the LHRH agonist ICI 118630 (Zoladex®). *J Endocrinol*. 1984;103(2):R1–4.
4. Kappy M, Stuart T, Perelman A, Clemons R. Suppression of gonatropin-secretion by a long-acting gonatropin-releasing hormone analog (Leuprolide acetate, Lupron depot) in children with precocious puberty. *J Clin Endocrinol Metab*. 1989;69(5):1087–9.
5. Owens DE, Peppas NA. Opsonization, biodistribution, and pharmacokinetics of polymeric nanoparticles. *Int J Pharm*. 2006;307(1):93–102.
6. Betancourt T, Byrne JD, Sunaryo N, Crowder SW, Kadapakkam M, Patel S, et al. PEGylation strategies for active targeting of PLA/PLGA nanoparticles. *Journal of Biomedical Materials Research Part A*. 2009;91A(1):263–76.
7. Meng FH, Engbers GHM, Feijen J. Polyethylene glycol-grafted polystyrene particles. *Journal of Biomedical Materials Research Part A*. 2004;70A(1):49–58.
8. Hermanson GT. *Bioconjugate Techniques*. Bioconjugate Techniques (Second Edition). 2 ed. New York: Academic Press; 2008.
9. Wattendorf U, Merkle HP. PEGylation as a tool for the biomedical engineering of surface modified microparticles. *J Pharm Sci*. 2008;97(11):4655–69.
10. Davis SS, Illum L, Neal JC, Garnett MC, Stolnik S. Modification of the copolymers poloxamer 407 and poloxamine 908 can affect the physical and biological properties of surface modified nanospheres. *Pharm Res*. 1998;15(2):318–24.
11. Hamad I, Al-Hanbali O, Hunter AC, Rutt KJ, Andresen TL, Moghimi SM. Distinct polymer architecture mediates switching of complement activation pathways at the nanosphere-serum interface: implications for stealth nanoparticle engineering. *ACS Nano*. 2010;4(11):6629–38.
12. Neal JC. *In vitro* displacement by rat serum of adsorbed radiolabeled poloxamer and poloxamine copolymers from model and biodegradable nanospheres. *J Pharm Sci*. 1998;87(10):1242–8.
13. Halperin A. Polymer brushes that resist adsorption of model proteins: a design parameters. *Langmuir*. 1999;15(7):2525–33.
14. Esmacili F, Ghahremani MH, Esmacili B, Khoshayand MR, Atyabi F, Dinarvand R. PLGA nanoparticles of different surface properties: preparation and evaluation of their body distribution. *Int J Pharm*. 2008;349(1–2):249–55.

15. Chan JM, Zhang L, Yuet KP, Liao G, Rhee J-W, Langer R, *et al.* PLGA-lecithin-PEG core-shell nanoparticles for controlled drug delivery. *Biomaterials*. 2009;30(8):1627–34.
16. Betancourt T, Shah K, Brannon-Peppas L. Rhodamine-loaded poly(lactic-co-glycolic acid) nanoparticles for investigation of *in vitro* interactions with breast cancer cells. *J Mater Sci: Mater Med*. 2009;20(1):387–95.
17. Fischer S, Foerg C, Ellenberger S, Merkle HP, Gander B. One-step preparation of polyelectrolyte-coated PLGA microparticles and their functionalization with model ligands. *J Control Release*. 2006;111(1–2):135–44.
18. Liu Y, Li K, Liu B, Feng S-S. A strategy for precision engineering of nanoparticles of biodegradable copolymers for quantitative control of targeted drug delivery. *Biomaterials*. 2010;31(35):9145–55.
19. Farokhzad OC, Cheng JJ, Teply BA, Sherifi I, Jon S, Kantoff PW, *et al.* Targeted nanoparticle-aptamer bioconjugates for cancer chemotherapy *in vivo*. *Proc Natl Acad Sci U S A*. 2006;103(16):6315–20.
20. Gref R, Minamitake Y, Peracchia MT, Trubetskoy V, Torchilin V, Langer R. Biodegradable long-circulating polymeric nanospheres. *Science*. 1994;263(5153):1600–3.
21. Gref R, Minamitake Y, Peracchia M, Trubetskoy V, Torchilin V, Langer R. Biodegradable long-circulating polymeric nanospheres. *Science*. 1994;263(5153):1600–3.
22. Andersen MO, Lichawska A, Arpanaci A, Jensen SMR, Kaur H, Oupický D, *et al.* Surface functionalisation of PLGA nanoparticles for gene silencing. *Biomaterials*. 2010;31(21):5671–7.
23. Torchilin VP. Micellar nanocarriers: pharmaceutical perspectives. *Pharm Res*. 2007;24(1):1–16.
24. Wang Y, Wang R, Lu X, Lu W, Zhang C, Liang W. Pegylated phospholipids-based self-assembly with water-soluble drugs. *Pharm Res*. 2010;27(2):361–70.
25. Goodwin J. *Colloids and Interfaces with Surfactants and Polymers: An Introduction*. West Sussex: John Wiley & Sons; 2004.
26. Shin S-B, Cho H-Y, Kim D-D, Choi H-G, Lee Y-B. Preparation and evaluation of tacrolimus-loaded nanoparticles for lymphatic delivery. *Eur J Pharm Biopharm*. 2010;74(2):164–71.